Journal of Applied Polymer Science

Alternative procedure for the incorporation of quantum dots into poly(*N*-isopropyl acrylamide-*co*-acrylic acid) microgels based on multiple interactions

Yuting Cai,[1] Xiaoqing Wu,[1] Qinghao Liu,[2] Hongyan Liu[3]

[1]School of Science, North University of China, Taiyuan 030051 Shanxi Province, People's Republic of China

[2]School of Chemical Engineering and Environment, North University of China, Taiyuan 030051, Shanxi Province, People's Republic of China

[3]Institute of Plant Protection, Henan Academy of Agricultural Sciences, Zhengzhou 450002, Henan Province, People's Republic of China

Correspondence to: Q. Liu (E-mail: liuqinghao0205@126.com)

ABSTRACT: Monodisperse fluorescent poly(*N*-isopropyl acrylamide-*co*-acrylic acid) microgels doped with quantum dots (QDs) were fabricated as follows. First, cysteamine-capped cadmium telluride (CA–CdTe) QDs were introduced into the microgels at pH 7 by electrostatic interactions. Afterward, the CA–CdTe QDs were further immobilized in the microgels by the collapse of the polymer network when the pH of solution was adjusted to 4. In this system, there existed multiple interactions between the CA–CdTe QDs and the microgels, including hydrogen bonds, electrostatic interactions, and coordination bonds. The photoluminescence intensity and maximum emission wavelength of the resulting microgels could be easily adjusted by changes in the content of the CA–CdTe QDs in the hybrid microgels (HMs) and with differently sized QDs, respectively. We found that the lower the addition of CA–CdTe QDs was, the bigger the blueshift of the photoluminescence spectra of the HMs was and the weaker the photoluminescence intensity was. Finally, temperature-responsive emission of the HMs was examined. © 2015 Wiley Periodicals, Inc. J. Appl. Polym. Sci. **2016**, *133*, 43227.

KEYWORDS: composites; microgels; self-assembly

Received 7 September 2015; accepted 11 November 2015

DOI: 10.1002/app.43227

INTRODUCTION

Hybrids of quantum dots (QDs) with microgels have great potential in diagnostics, bioimaging, photonics, optoelectronics, catalysis, and sensors.[1] A number of methods have been developed to fabricate such hybrid materials. For example, microgels have been used as templates for the *in situ* synthesis of QDs; microgels enable the flexible control of the loading of QDs. However, the obtained QDs in microgels are usually polycrystalline and show a broad size distribution; this results in the poor control of the photoluminescence (PL) of the hybrid microgels (HMs).[2–4] In another method, microgels are loaded with preformed QDs through specific interactions, including electrostatic interactions,[5–7] hydrogen bonding,[8] hydrophobic forces,[9–11] covalent bonds,[12–14] physical entanglement of polymer chains,[15,16] ligand exchange between QDs and microgels.[17] Thus, the QD size and optical properties are independently adjusted before they are loaded into microgels.

Responsive microgels have been used to create hybrids with controlled fluorescent properties. For example, Wang *et al.*[16] demonstrated the use of pH-sensitive poly(*N*-isopropyl acrylamide-*co*−4-vinyl pyridine) microgels to take up thioglycolic acid-capped cadmium telluride (CdTe) QDs. The QDs were absorbed into the swollen microgels at low pH. Afterward, the microgels collapsed with an increase in pH to above the pK_a of 4-vinyl pyridine groups (5.39) and, thus, trapped the QDs. During this process, the physical entanglement of the collapsed network and the electrostatic interactions between the loaded QDs and the microgel network played an important role in the entrapment of QDs in the microgels. However, the electrostatic interactions here existed only in a relatively narrow range of pH, from 3.53[18] (the pK_a of carboxylic acid from thioglycolic acid-capped CdTe QDs) to 5.39, and the QDs were prone to leakage from the microgels at pHs beyond this range. The narrow pH range was mainly determined by the relatively small pK_a of the 4-vinyl pyridine group; this motivated us to replace the pyridine group

Additional Supporting Information may be found in the online version of this article.

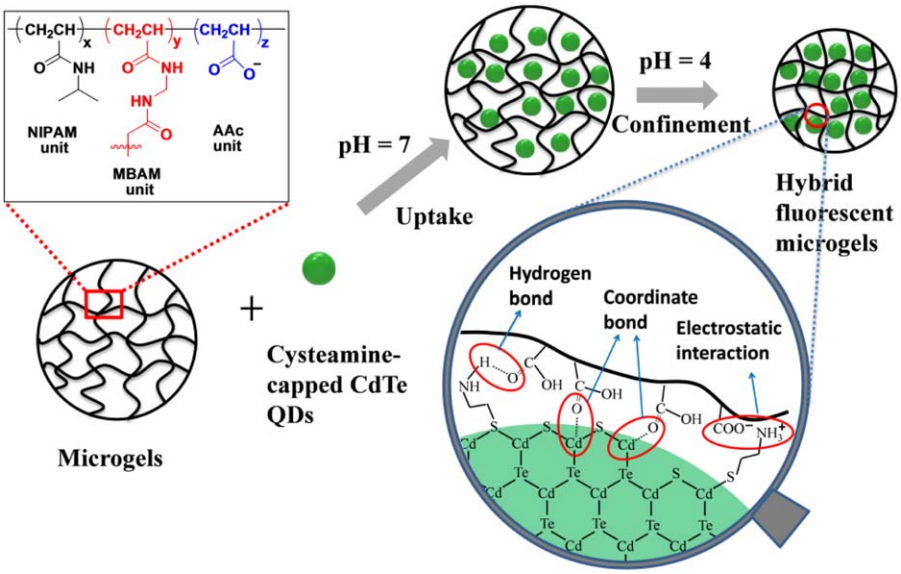

Figure 1. Scheme for the synthesis of the CdTe/poly(NIPAM-*co*-AAc) HMs and interactions between the microgels and CA–CdTe QDs. [Color figure can be viewed in the online issue, which is available at wileyonlinelibrary.com.]

with another group with a larger pK_a in this system to fabricate another kind of hybrid fluorescent microgel.

In this study, we demonstrated the use of poly(*N*-isopropyl acrylamide-*co*-acrylic acid) [poly(NIPAM-*co*-AAc)] microgels to adsorb and stabilize cysteamine-capped cadmium telluride (CA–CdTe) QDs; this resulted in hybrid-fluorescent-microgel-based multiple interactions (Figure 1). Herein, the acrylic acid (AAc) monomer was used to synthesize pH-responsive poly(NIPAM-*co*-AAc) microgels because it was negatively charged at pHs above the pK_a of the carboxyl group from poly(NIPAM-*co*-AAc) microgels (~4.25)[19] and became neutral below the pK_a. On the other hand, the CA–CdTe QDs carried positive charges at pHs lower than the pK_a (8.3) of the primary amine from cysteamine hydrochloride (CA).[20] Such pH-responsive behavior allowed for convenient control of the charges and swelling behavior of the microgels, which were used to encapsulate and stabilize the CA–CdTe QDs. What is more, the CdTe/poly(NIPAM-*co*-AAc) HMs synthesized by this method showed reversible, temperature-responsive emission properties.

EXPERIMENTAL

Materials

Cadmium chloride ($CdCl_2 \cdot 2.5H_2O$), tellurium powder (100 mesh, 99.999%), sodium borohydride ($NaBH_4$; 96%), and ammonium persulfate were purchased from Sinopharm Chemical Reagent Shanghai Co., Ltd. CA (98%), *N*-isopropyl acrylamide (NIPAM; 98%), *N*,*N*′-methylene bisacrylamide (MBAM; 95%), and AAc (>99%) were purchased from Aladdin Reagent Co. NIPAM was purified by recrystallization from a toluene/hexane mixture (50/50% vol). AAc was purified by distillation under reduced pressure to remove the hydroquinone inhibitor before use. Deionized water was used during the syntheses and measurements.

Preparation of Sodium Hydrogen Telluride (NaHTe)

$NaBH_4$ was used to react with tellurium with a molar ratio of 5:1 in water to produce NaHTe.[21] Briefly, 2 mL of deionized water was transferred to a small flask. Then, 51.6 mg of tellurium powder and 74.6 mg of $NaBH_4$ were added, and the reacting system was kept at 4°C. During the reaction, a small outlet connected to the flask was kept open to discharge the pressure from the resulting H_2. After approximately 8 h, the black tellurium powder disappeared, and a white sodium tetraborate precipitate appeared on the bottom of the flask instead. The resulting NaHTe in the clear supernatant was used for the preparation of the CA–CdTe QDs.

Synthesis of the CA–CdTe QDs

Water-soluble CA–CdTe QDs were synthesized according to a previously published method.[22] A series of aqueous colloidal CA–CdTe QD solutions was prepared with different refluxing times by the addition of 1 mL of fresh NaHTe solution to 100 mL of 4 mmol/L N_2-saturated $CdCl_2$ solutions at pH 4.8 in the presence of CA as a stabilizing agent. The Cd^{2+}/stabilizer/HTe^- molar ratio was fixed at 1:2.4:0.5. The resulting mixture was refluxed to control the growth of the CdTe QDs. The sizes of the QDs mentioned in this article were calculated with Peng's empirical equation and were used to define the QDs unless otherwise specified.

Synthesis of the Poly(NIPAM-*co*-AAc) Microgels

The poly(NIPAM-*co*-AAc) microgels were synthesized with a modified route.[23] Briefly, 1.5 g of NIPAM, 0.03 g of MBAM, and 0.15 mL of AAc were dissolved in 45 mL of filtered, deionized water in a three-necked flask equipped with a magnetic stirring bar and purged with N_2 for 1 h. A volume of 30 mL of this solution was then transferred into a constant-pressure dropping funnel. A volume of 15 mL of water and an amount of 0.1 g of NIPAM were added to the remaining 15-mL solution in the flask, and the liquid was heated to 70°C with an N_2 purge. The polymerization was initiated by the addition of

Table I. Recipes for the Syntheses of HMs

Code	CdTe (2.5 nm; mL)	CdTe (2.7 nm; mL)	CdTe (3.2 nm; mL)	Microgel (mL)
HM4-0	4	0	0	25
HM3-1	3	0	1	25
HM2-2	2	0	2	25
HM0-4	0	0	4	25
HM2.50	0	2.50	0	25
HM3.25	0	3.25	0	25
HM4.00	0	4.00	0	25

The concentration of the CA-CdTe QDs was 4 mmol/L (this refers to the concentration of Cd in this article).

0.02 g of ammonium persulfate dissolved in 2 mL of water. The solution started to become turbid in 2 min and was then fed with the solution in the constant-pressure dropping funnel at 1 mL/min. After all of the solution was added, the reaction was continued for another 4 h before it was cooled down rapidly in an ice bath. After cooling, the microgels were purified by at least three cycles of ultracentrifugation at 15,000 rpm for 20 min, decantation, and redispersion in deionized water.

Encapsulation of the CA–CdTe QDs in the Poly(NIPAM-*co*-AAc) Microgels

A series of samples was prepared according to the recipes given in Table I. Briefly, at room temperature, a 25-mL dispersion of microgels (solid content = 0.7 mg/mL) was mixed with a certain amount of CA–CdTe QD aqueous solution at pH 7 under stirring. After incubation for 10 min, the pH of the mixed solution was adjusted to 4 by the addition of dilute sulfuric acid. Then, the solution was centrifuged at 14,000 rpm for 20 min. The unloaded CA–CdTe QDs were removed, and microgels loaded with CA–CdTe QDs were obtained in a sulfuric acid solution at pH 4; this was denoted as CdTe/poly(NIPAM-*co*-AAc). The solid content of all of the HM solutions that were used for the measurements was 0.8 mg/mL.

Characterization and Measurements

All of the samples that were used for measurements were dialyzed against deionized water for 3 days with the dialysis water refreshed three times a day. The chemical structure of the CA–CdTe QDs was characterized with a Nicolet 6700 Fourier transform infrared (FTIR) spectrometer (Thermo Fisher Scientific) with scanning from 400 to 4000 cm^{-1} at a resolution of 4 cm^{-1}. The crystal structure of the QDs was characterized with a D8 Advance X-ray diffractometer (Bruker AXS, Germany). The diluted HM dispersion was dropped onto carbon-coated copper grids and dried at room temperature for transmission electron microscopy (TEM) imaging with a 2100 transmission electron microscope (JEOL, Japan) at 200 kV. Energy-dispersive X-ray was used to investigate the elemental composition of the CdTe/poly(NIPAM-*co*-AAc) microgels. The ζ potential of the CA–CdTe QDs and the hydrodynamic diameters of the pure hydrogels and HMs dispersed in pH 4 solutions were measured with a Zetasizer Nano ZS dynamic light scattering instrument (Malvern, United Kingdom) at 25°C. The ultraviolet–visible (UV–vis) absorption and PL spectra were obtained with a Lambda 950 UV–vis spectrometer (PerkinElmer) and a Hitachi F-4600 fluorescence spectrophotometer, respectively.

RESULTS AND DISCUSSION

Characterization of the CA–CdTe QDs

Figure 2 shows the UV–vis absorption and PL spectra of the obtained CA–CdTe QDs synthesized with different refluxing times. With the extension of refluxing time, the absorbance peak was shifted to the long-wavelength side; this indicated the growth of the CA–CdTe QDs over time. The emission peak of the CA–CdTe QDs also gradually shifted to the long-wavelength side because of the quantum confinement effect, and the PL intensity increased gradually. The mean particle size was estimated according to calculations based on the adsorption peak with Peng's empirical equation.[24] These values were very close to those measured by TEM. For example, the CA–CdTe QDs prepared with refluxing for 7 h showed an average size of about 3.6 nm, as shown in the TEM image [Figure 3(A,B)]; this was close to the calculated value (3.2 nm). Similarly, the average sizes of the CA–CdTe QDs synthesized with refluxing times of 1 and 3 h were 2.5 and 2.7 nm, respectively, according to Peng's empirical equation. For convenience, the mean size of the CA–CdTe QDs mentioned in the following part refers to the value calculated from Peng's empirical equation unless otherwise specified.

These QDs were crystalline. For example, the powder of the CA–CdTe QDs obtained with a refluxing time of 7 h showed characteristic diffractions of a cubic zinc blend structure at 23.9, 39.8, and 46.1° [Figure 3(C)]. The average crystal size of the QDs determined by Debye–Scherrer's formula was about 3.2 nm.

The surface chemistry of the CA–CdTe QDs was investigated with FTIR spectroscopy. The IR spectra of the CA·HCl and CA–CdTe QDs are shown in Figure 3(D). For CA·HCl, the bands at 2600–2500 cm^{-1} were assigned to the stretching vibrations of S—H. The bands at 3500–3000 cm^{-1} were related to the stretching vibrations of O—H (H_2O) and N—H (—NH_2).

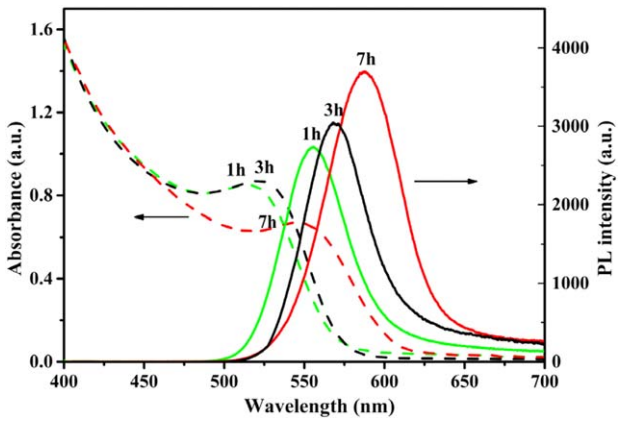

Figure 2. Temporal evolution of the absorption and PL spectra of the CA–CdTe QDs synthesized with different refluxing times. [Color figure can be viewed in the online issue, which is available at wileyonlinelibrary.com.]

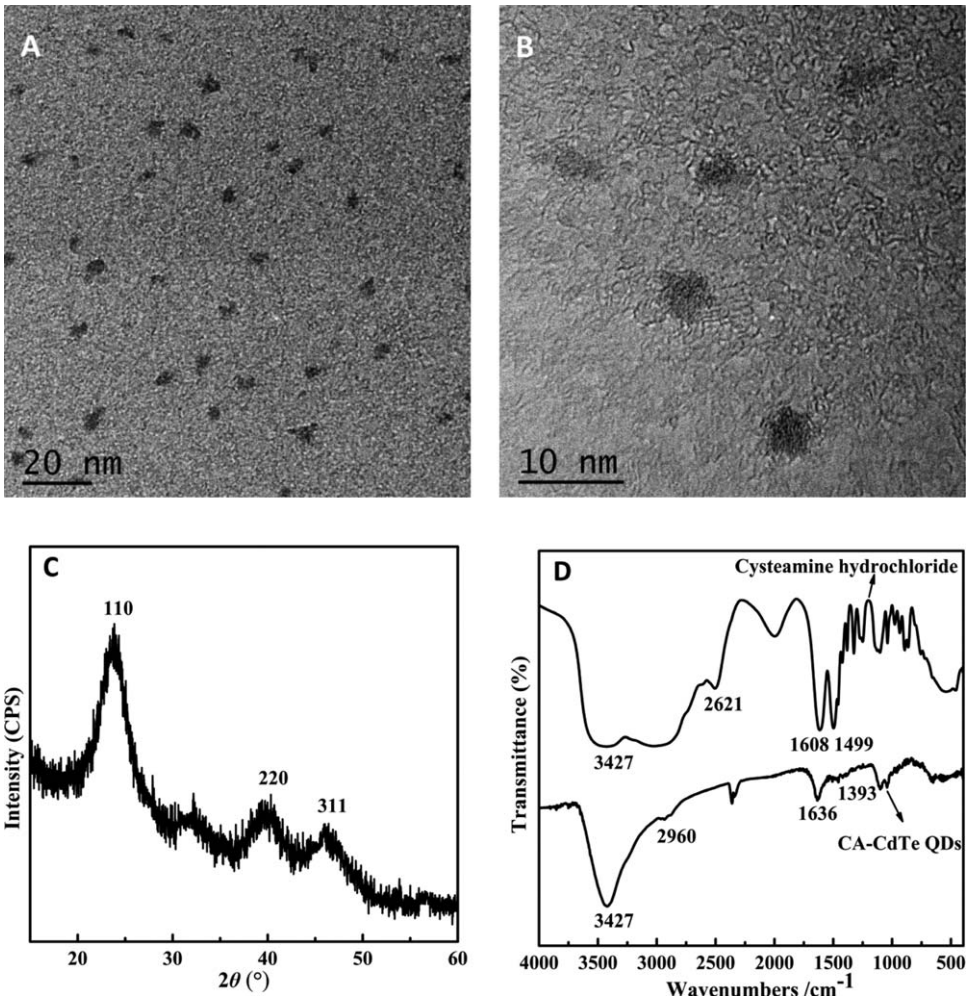

Figure 3. (A) TEM image, (B) enlarged TEM image, (C) X-ray diffraction spectrum, and (D) FTIR spectrum of the CA–CdTe QDs synthesized with a refluxing time of 7 h.

For CA–CdTe QDs, no absorption at 2600–2500 cm^{-1} was observed; this suggested that —SH in CA was covalently bound on the QD surface. In addition, the broad bands at 3300–3000 cm^{-1} in the CA–CdTe QDs almost disappeared. This was the result of more —NH_2 exposed on the QD surface; this was illuminated by a much narrower absorption band around 3400 cm^{-1}. These results confirmed the surface modification of the QDs with the CA molecules.

Such surface modification of the CA molecules entitled positive surface charges on the QDs at pH 7. Hereafter, the positively charged CA–CdTe QDs were used in the composites with negatively charged microgels through electrostatic interactions.

Syntheses and Characterization of the Poly(NIPAM-*co*-AAc) Microgels and QD/Microgel Composites

The microgels used in this study were prepared by a semibatch method.[23,25–28] The optical micrograph of the microgels in Figure 4 reveals an average size of 1.4 μm with a narrow polydispersity. The chemical structure was qualitatively characterized by FTIR spectroscopy (Figure S1, Supporting Information; electronic supporting information (ESI)). The band at 1648 cm^{-1} was assigned to the stretching vibrations of C═O. The band at 1549 cm^{-1} was related to the in-plane bending vibrations of N—H. The band at 1713 cm^{-1} was related to the ester carboxyl group, and the bands at 1389 and 1369 cm^{-1} were attributed to symmetrical bending vibrations and a coupling split originating from the dimethyl of the isopropyl group, respectively. These results indicate the formation of copolymers.

The AAc, a weak acid, moieties of the microgels rendered microgels with pH sensitivity. When the pH of the solution was higher than the apparent pK_a of AAc (~4.25),[19] the AAc groups of the poly(NIPAM-*co*-AAc) microgels carried negative charges because of the deprotonation of AAc; this led to internal electrostatic repulsion between the deprotonated AAc groups and thus caused a swelling of the poly(NIPAM-*co*-AAc) microgels. Otherwise, the AAc groups were less ionized, and the polymer–polymer interactions became dominant; this led to a collapse of the poly(NIPAM-*co*-AAc) microgels.

To load the CA–CdTe QDs into the poly(NIPAM-*co*-AAc) microgels, the CA–CdTe QDs were mixed with microgels and incubated at pH 7 for 30 min. Subsequently, the pH of solution was adjusted to 4 to collapse the microgels. Thus, we supposed that the QDs were trapped in the microgels, as illustrated in

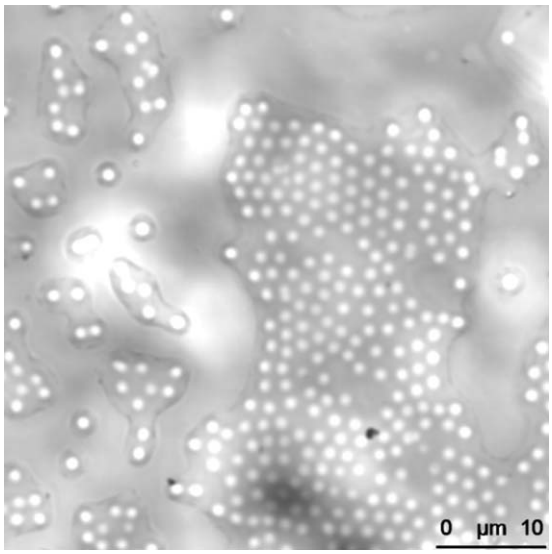

Figure 4. Optical micrograph of the poly(NIPAM-*co*-AAc) microgels.

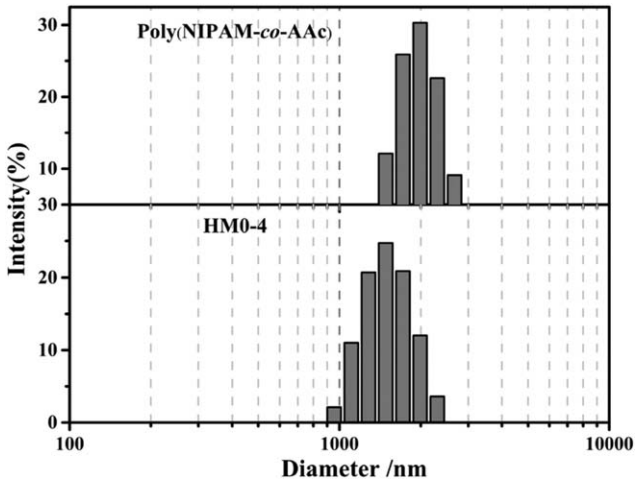

Figure 6. Dynamic light scattering histograms of the poly(NIPAM-*co*-AAc) microgels and the HM0–4 sample determined at 25°C and pH 4.

Figure 1. The volume ratio of the CA–CdTe QD dispersion to the poly(NIPAM-*co*-AAc) microgel dispersion was varied from 0.10 to 0.16. In the other part, the volume ratio was fixed to 0.16, and differently sized CA–CdTe QDs were used. The obtained suspension was ultracentrifuged, and the supernatant was decanted. The sediment emitted fluorescence under UV irradiation; this indicated successful loading of the CA–CdTe QDs in the poly(NIPAM-*co*-AAc) microgels.

When the microgels were composited with QDs, the UV absorbance and the PL of the QDs were blueshifted (Figure 5). The 2.7-nm CA–CdTe QDs showed an absorbance at 520 nm. As incorporated into microgels, the peak bands were shifted to 514, 510, and 509 nm when the additions of QDs were 4.00, 3.25, and 2.5 mL, respectively [Figure 5(A)]. Meanwhile, the PL peak shifted from 569 nm to 559, 557, and 556 nm [Figure 5(B)], whereas the PL intensity decreased (the results are not shown here).

Such blueshifted PL was likely caused by the decrease in the size of the CdTe QDs. Within the microgel, the AAc groups chemically etched the surface of the CdTe QDs; this led to the formation of a CdO layer when Cd was coordinated with the carboxyl groups.[18,29] The degree of etching was dependent on the ratio of CdTe QDs to microgels. A lower Cd/AAc ratio likely resulted in a higher size decrease, and this to a greater blueshift of the emission peak. This AAc etching is schematically illustrated in Figure 1. In addition to the electrostatic interactions and hydrogen bonds between the QDs and microgels, it was likely that AAc/Cd coordination may have been another important tie of the poly(NIPAM-*co*-AAc) chains to the CA–CdTe QDs.

With such multiple interactions, the hydrodynamic diameter of the microgels decreased. Dynamic light scattering was used to determine the hydrodynamic diameters of the HMs in solution at 25°C (Figure 6). The results show that the average hydrodynamic diameter of HM0–4 was about 1531 nm; this was smaller than that of the pure microgels (2417 nm). In these composite microgels, the CA–CdTe QDs served as local crosslinkers.

TEM was used to image the CdTe/poly(NIPAM-*co*-AAc) microgels. The size of HM0–4 under TEM was about 920 nm [Figure 7(A)]; this was significantly smaller than the dynamic light scattering value, probably because of the shrinkage of HMs during

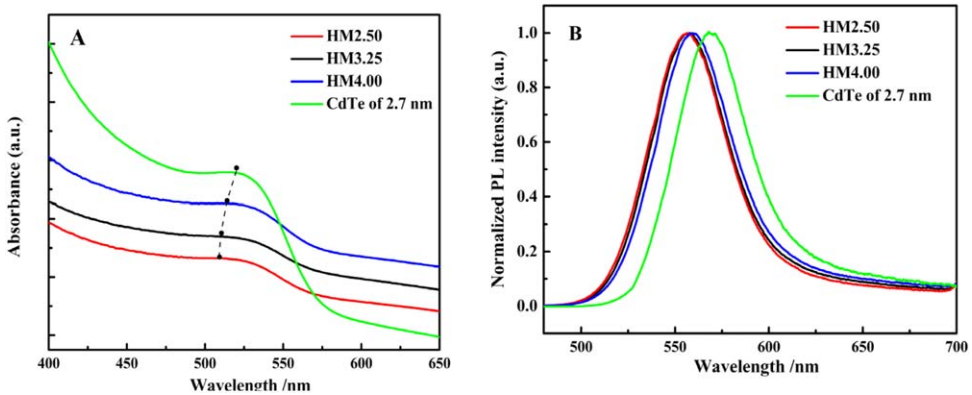

Figure 5. (A) Absorption and (B) PL spectra of different HMs. [Color figure can be viewed in the online issue, which is available at wileyonlinelibrary.com.]

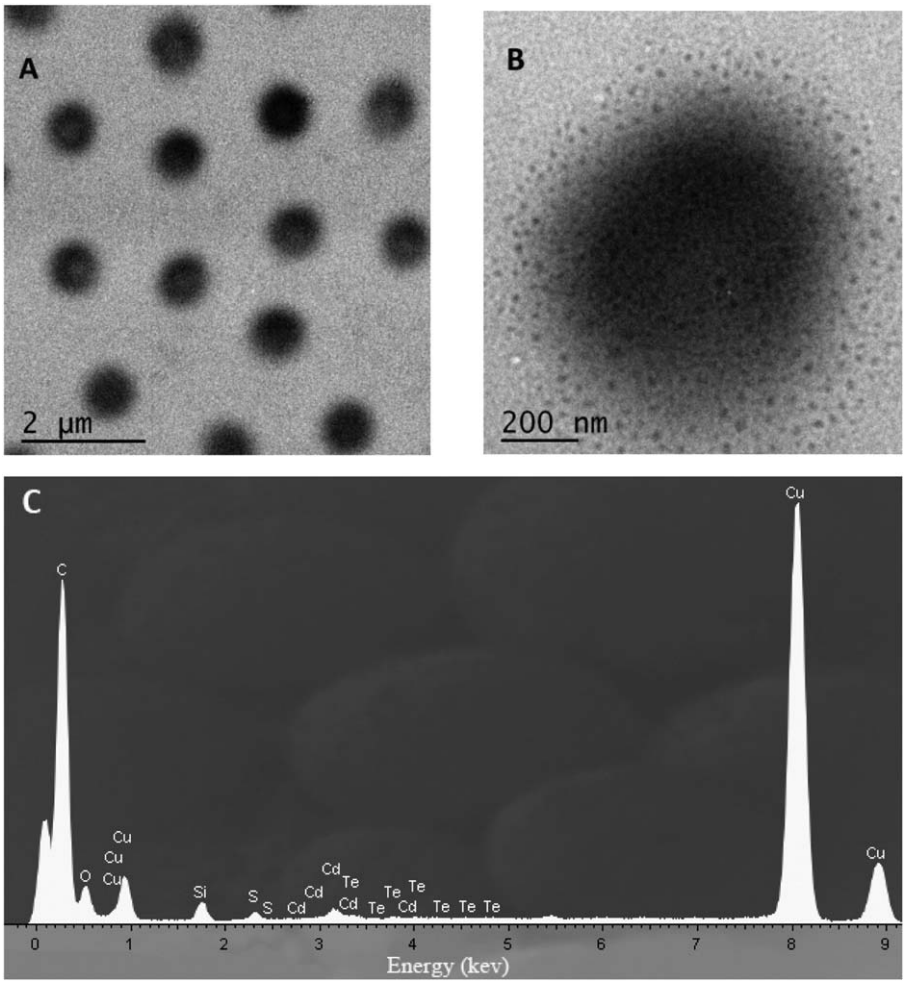

Figure 7. (A) TEM image, (B) enlarged TEM image, and (C) energy-dispersive X-ray spectrum of the HM0–4 sample.

dehydration. The CA–CdTe QDs were well distributed in the microgel matrix [Figure 7(B)]. In addition, the QDs were found as aggregates, with an average size of about 20 nm; this was larger than the single CA–CdTe QDs. This may have been caused by the collapse of the microgels during the adjustment of the pH of the solution. To further identify the presence of the CdTe QDs, electron-dispersive spectroscopy was performed on the microgels; this showed the abundant presence of Cd and Te atoms [Figure 7(C)].

Apparently, such a facile and versatile method for incorporating QDs into microgels could be applied for QDs with different sizes and different PLs. For example, CdTe QDs of 2.5 and 3.2 nm, the fluorescent image of which are presented in Figure 8(A), were separately incorporated into the microgels. These nanocomposite microgels appeared green [Figure 8(B)] and yellow [Figure 8(E)] under UV irradiation, respectively. Moreover, pure microgels were incubated with a mixture of 2.5-nm (green) and 3.2-nm (yellow) CdTe QDs (the ratio of the two kinds of CA–CdTe QDs was different). After the removal of excess CdTe QDs, distinctive emission colors of the resulting HMs were obtained [Figure 8(C,D)]. The emission peak position was dependent on the ratio of the two kinds of QDs. Thus, it was convenient to control the maximum emission wavelength of the HMs through the adjustment of the ratio of differently sized CdTe QDs [Figure 8(F)]. On the other hand, because of the higher fluorescent quantum yield of CA–CdTe QDs of 3.2 nm compared to that of the CA–CdTe QDs of 2.5 nm, the PL intensity of the HMs gradually increased with the increasing proportion of CA–CdTe QDs of 3.2 nm [Figure 8(B–E)]. These results suggest an excellent preparation strategy for HMs with different fluorescences. On the basis of such a versatile synthesis of the QD/microgel hybrid, it was natural to anticipate the preparation of similar functional HMs by a smart combination of functional moieties with responsive microgels.

In addition, the CdTe/poly(NIPAM-*co*-AAc) HMs showed distinctive temperature-responsive emission behavior compared to the CA–CdTe QD solution. Figure 9(A,B) depicts the PL spectra of the HMs of HM4–0 and the CA–CdTe QDs of 2.5 nm carried out in the temperature range from 15 to 55°C, respectively. When the temperature increased, the PL intensity of HM4–0 and CA–CdTe QDs both gradually weakened, but the PL intensity of HM4–0 changed rapidly compared to that of the CA–CdTe QDs, as shown in Figure 9(C). Scattering caused by a microgel volume transition on heating was the main reason for the decrease in the PL intensity of the HMs.[30] On the other hand, a redshift of the PL spectra was observed when the

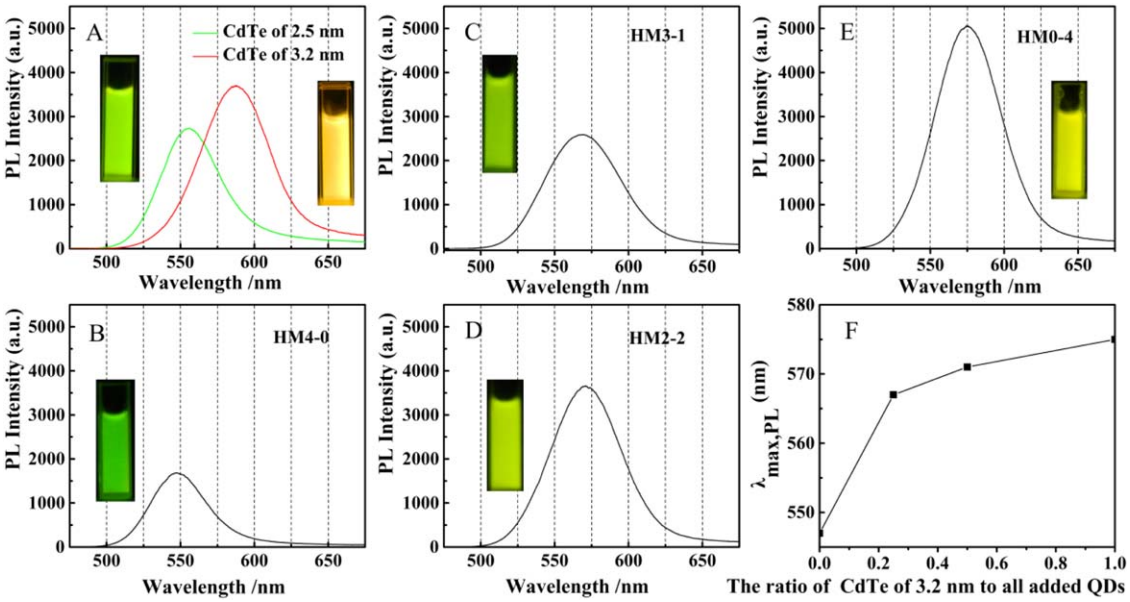

Figure 8. Fluorescence spectra of (A) CdTe (2.5 and 3.2 nm), (B) HM4–0, (C) HM3–1, (D) HM2–2, and (E) HM0–4. (F) Relationship of the ratio of CdTe (3.2 nm) to all of the added QDs and PL peak. The insets show the corresponding fluorescence images of the QDs and HMs. $\lambda_{max,PL}$, maximum emission wavelength of the PL spectrum. [Color figure can be viewed in the online issue, which is available at wileyonlinelibrary.com.]

temperature increased. This result correlated well with those obtained by Li *et al.*[30]

Furthermore, we demonstrated that the PL intensities and maximum emission peak wavelengths responding to the temperature were reversible. When the temperature was down to 15°C, the emission peaks shifted rapidly back to their original positions from their positions at 55°C. The reversibility of the responses from these CdTe/poly(NIPAM-*co*-AAc) HMs to temperature [seen in Fig. 9(D)] made it possible to develop a QD-based thermosensitive device or sensor.

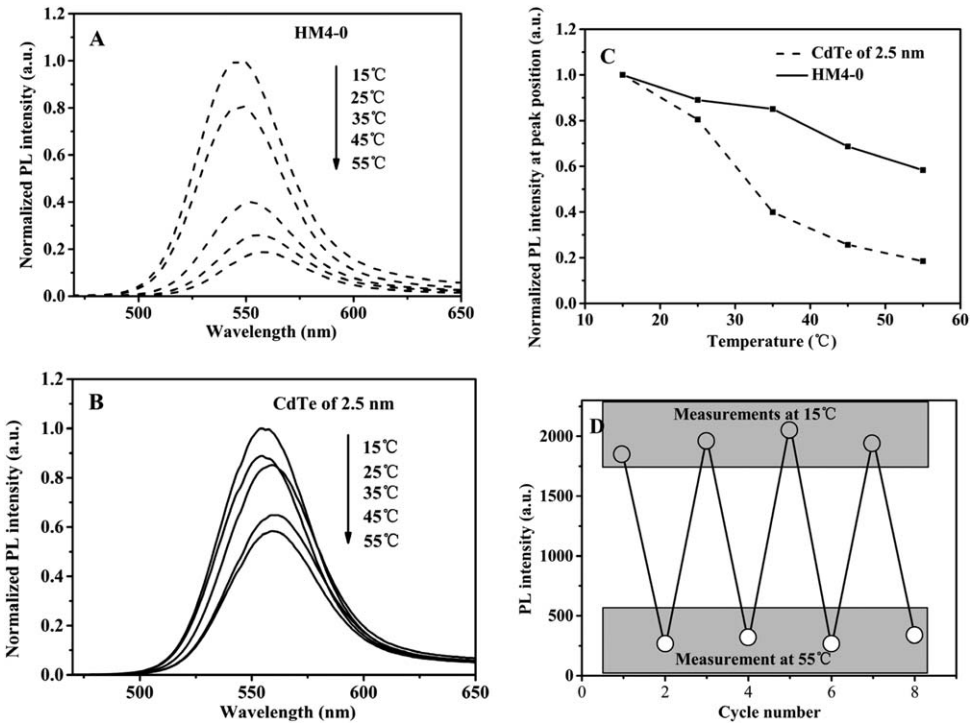

Figure 9. PL spectra of (A) HM4–0 and (B) CdTe (2.5 nm) taken at different temperatures, (C) PL intensity at PL maximum wavelengths as a function of temperature, and (D) PL intensity measured during repeated heating (55°C) and cooling (15°C) cycles for HM4–0.

CONCLUSIONS

In this study, poly(NIPAM-*co*-AAc) microgels doped with CA–CdTe QDs were fabricated on the basis of multiple interactions, including hydrogen bonds, coordinate bonds, and electrostatic interactions. This method was demonstrated to be versatile for the encapsulation of differently sized CA–CdTe QDs and was used to easily fabricate PL microgels with tunable colors. In addition, such HMs had temperature-responsive emission behavior, and its PL intensity became weak with increasing temperature. Such HMs may find applications in thermosensitive devices and sensors.

ACKNOWLEDGMENTS

This work was supported by the China Agriculture Research System (contract grant number CARS-15-1-05).

REFERENCES

1. Sahiner, N.; Sagbas, S.; Yoshida, H.; Lyon, L. A. *Colloids Interface Sci. Commun.* **2014**, *2*, 15.
2. Cang, Y.; Zhang, R.; Shi, G.; Zhang, J.; Liu, L.; Hou, X.; Yu, Z.; Fang, D.; Guo, X. *J. Mater. Chem. C* **2015**, *3*, 3745.
3. Wu, W.; Zhou, T.; Shen, J.; Zhou, S. *Chem. Commun.* **2009**, 4390.
4. Wu, W. T.; Zhou, T.; Aiello, M.; Zhou, S. Q. *Biosens. Bioelectron.* **2010**, *25*, 2603.
5. Yoo, J. H.; Lee, S. W. *J. Nanosci. Nanotechnol.* **2014**, *14*, 7648.
6. Gui, R.; An, X.; Gong, J.; Chen, T. *Mater. Lett.* **2012**, *88*, 122.
7. Li, J.; Liu, B.; Li, J. *Langmuir* **2006**, *22*, 528.
8. Gong, Y.; Gao, M.; Wang, D.; Möhwald, H. *Chem. Mater.* **2005**, *17*, 2648.
9. Janczewski, D.; Tomczak, N.; Han, M. Y.; Vancso, G. J. *Eur. Polym. J.* **2009**, *45*, 1912.
10. Janczewski, D.; Tomczak, N.; Han, M. Y.; Vancso, G. J. *Macromolecules* **2009**, *42*, 1801.
11. Jańczewski, D.; Tomczak, N.; Song, J.; Long, H.; Han, M.-Y.; Vancso, G. J. *J. Mater. Chem.* **2011**, *21*, 6487.
12. Wang, L.; Sun, J. *J. Mater. Chem.* **2008**, *18*, 4042.
13. Agrawal, M.; Rubio-Retama, J.; Zafeiropoulos, N. E.; Gaponik, N.; Gupta, S.; Cimrova, V.; Lesnyak, V.; López-Cabarcos, E.; Tzavalas, S.; Rojas-Reyna, R.; Eychmüller, A.; Stamm, M. *Langmuir* **2008**, *24*, 9820.
14. Liu, J. B.; Yang, X. H.; Wang, K. M.; Wang, Q.; Ji, H. N.; Wu, C. L.; Li, J.; He, X. X.; Tang, J. L.; Huang, J. *J. Mater. Chem.* **2012**, *22*, 495.
15. Wang, Y.-Q.; Zhang, Y.-Y.; Zhang, F.; Li, W.-Y. *J. Mater. Chem.* **2011**, *21*, 6556.
16. Kuang, M.; Wang, D.; Bao, H.; Gao, M.; Möhwald, H.; Jiang, M. *Adv. Mater.* **2005**, *17*, 267.
17. Shen, L.; Pich, A.; Fava, D.; Wang, M. F.; Kumar, S.; Wu, C.; Scholes, G. D.; Winnik, M. A. *J. Mater. Chem.* **2008**, *18*, 763.
18. Zhang, H.; Zhou, Z.; Yang, B.; Gao, M. Y. *J. Phys. Chem. B* **2003**, *107*, 8.
19. Islam, M.; Ahiabu, A.; Li, X.; Serpe, M. *Sensors Basel* **2014**, *14*, 8984.
20. Bonengel, S.; Bernkop-Schnurch, A. *J. Controlled Release* **2014**, *195*, 120.
21. Hao, E.; Zhang, H.; Yang, B.; Ren, H.; Shen, J. *J. Colloid Interface Sci.* **2001**, *238*, 285.
22. He, Y.; Yin, P.; Gong, H.; Peng, J.; Liu, S.; Fan, X.; Yan, S. *Sens. Actuators B* **2011**, *157*, 8.
23. Still, T.; Chen, K.; Alsayed, A. M.; Aptowicz, K. B.; Yodh, A. G. *J. Colloid Interface Sci.* **2013**, *405*, 96.
24. Chen, J.; Zheng, A.; Gao, Y.; He, C.; Wu, G.; Chen, Y.; Kai, X.; Zhu, C. *Spectrochim. Acta A* **2008**, *69*, 1044.
25. Zhang, Q.; Zha, L.; Ma, J.; Liang, B. *J. Colloid Interface Sci.* **2009**, *330*, 330.
26. Acciaro, R.; Gilanyi, T.; Varga, I. *Langmuir* **2011**, *27*, 7917.
27. Kwok, M.-H.; Li, Z.; Ngai, T. *Langmuir* **2013**, *29*, 9581.
28. Brijitta, J.; Tata, B. V. R.; Joshi, R. G. *J. Polym. Res.* **2015**, *22*, 36.
29. Yang, G.; Shen, P.; Tan, K.; Xia, Y. *Microchim. Acta* **2014**, *181*, 607.
30. Li, J.; Hong, X.; Liu, Y.; Li, D.; Wang, Y. W.; Li, J. H.; Bai, Y. B.; Li, T. *J. Adv. Mater.* **2005**, *17*, 163.